Compressed Sensing in MRI: how the Maximum Undersampling Factor depends on the Image Size

C. Lazarus[1], A. Coste[2], N. Chauffert[1], A. Vignaud[2], P. Ciuciu[1]

[1]Gif-sur-Yvette,FR,CEA,DRF/I2BM/NeuroSpin/UNATI/Parietal
[2]Gif-sur-Yvette,FR,CEA,DRF/I2BM/NeuroSpin/UNIRS

INTRODUCTION

Since the work of Lustig et al. on Sparse MRI [1], Compressed Sensing (CS) has promised great opportunities to drastically shorten the acquisition time in MRI by reconstructing images from undersampled Fourier data. Although CS theories provide upper bounds relating the number of required measurements m to the image sparsity and its number of pixels $N \times N$ to guarantee exact recovery in the noise-free case, in practice (noisy case) it remains unclear to what extent MRI acquisitions can be accelerated while preserving image quality. More precisely, finding the relationship linking the maximum achievable undersampling factor $R = N^2/m$ to the image size in a noisy context is still an open question. In this numerical and experimental study, we propose quantitative hints that may guide CS-MRI users in their choice of an appropriate undersampling factor as a function of image size and SNR (Signal to Noise Ratio).

MATERIALS AND METHODS

Which images?

- **2D brain simulated T2 weighted like images** for increasing image sizes (N=128, 256, 512, 1024, 2048) and noise levels characterized by their input ***SNR***, produced by adding complex Gaussian white noise with varying standard deviation to the Fourier data.
- $SNR = \frac{S}{\sigma}$ where S refers to the mean signal of a ROI taken in the white matter and σ to the standard deviation in the background signal in the amplitude image.

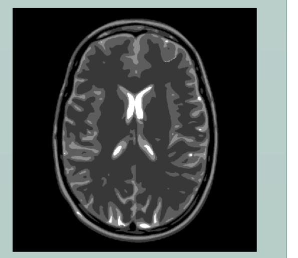

Which undersampling?

- Non-Cartesian samples were randomly picked in the Fourier space according to a variable density [2]
- Acceleration factors (R=5, 10, 20 and 30).

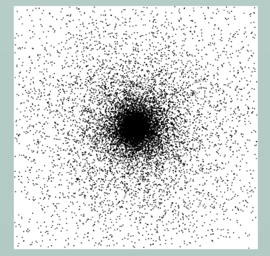

Which reconstruction?

- Nonlinear non-Cartesian reconstructions
- redundant wavelet transform from the RICE toolbox [5]
- NFFT [6]
- FISTA algorithm [3] for solving the penalized CS L_1-minimization problem with a constant $\lambda = 10^{-4}$

$$\underset{z}{minimize} \overbrace{\|Az - y\|_2^2}^{\text{Data consistency}} + \underbrace{\lambda\|z\|_1}_{\text{Enforces sparsity}}$$

$A = F\psi^{-1}$ *with* F the Fourier transform *and* ψ the sparsifying transform
y : acquired data ; x : image ; $z = \psi x$: sparse representation of x ;
λ : regularization parameter

Which image quality metrics?

- SSIM [4]: measuring the similarity in structure of image I with a full k-space reference image I_0. ($SSIM(I, I_0) = 1$ is a perfect match while $SSIM(I, I_0) = 0$ is a null correspondence).
  - For noise-free case: I_0=fully sampled image with infinite SNR.
  - For noisy case: I_0=fully sampled image with high SNR=105.

Experimental validation

- T2* weighted Cartesian 2D acquisitions (birdcage 1Tx/1Rx coil) of an ex-vivo brain baboon with our in-house 7T scanner for N=512 and different SNR (by signal averaging), resulting in a large set of experimental images $I_0(N, SNR)$ that we undersampled and reconstructed following the aforementioned method.

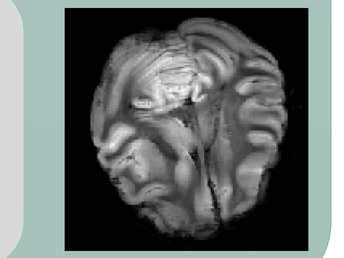

RESULTS AND DISCUSSION

Influence of image size

- At a fixed acceleration factor, SSIM is increasing with N, conveying the improvement of image quality.
- Two regimes can be identified (delimited by blue dot-line on Fig.1): while image quality is stationary for large image sizes (close to its maximum value of 1), it rapidly decreases for small decreasing values of N.
- Large acceleration factors are only achievable for large image sizes.

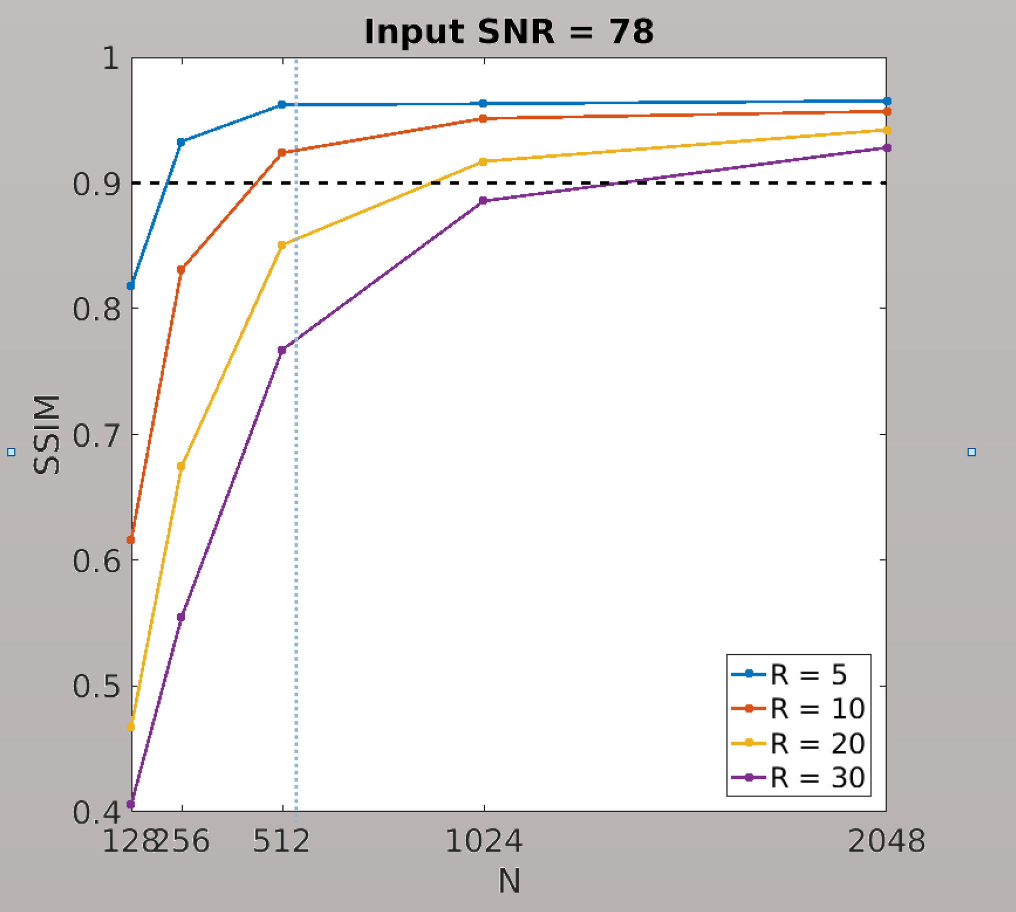

***Figure 1**: For a constant input SNR=78, evolution of SSIM as a function of image size N for four acceleration factors R=5 (blue), R=10 (orange), R=20 (yellow) and R=30 (purple). The black dashed line indicates a chosen SSIM threshold of 0.9.*

Influence of SNR

- For a constant image size, image quality scores are increasing with the input SNR.
- Given a targeted image quality characterized by a certain SSIM threshold (e.g. 0.9 on Fig. 2), only undersampling factors of 5 and 10 should be used for N=512. Moreover, the desired quality will only be reached if the input SNR is sufficiently high ($SNR > 40$).
- Experimental points (* in Fig. 2) seem to confirm the results obtained on simulated brain images, especially for R=5. For higher acceleration factors however (e.g. R=20), experimental scores are slightly larger than in simulations, especially for high SNR. The distinct natures of the two images and the different contribution of the black background may explain these variations.

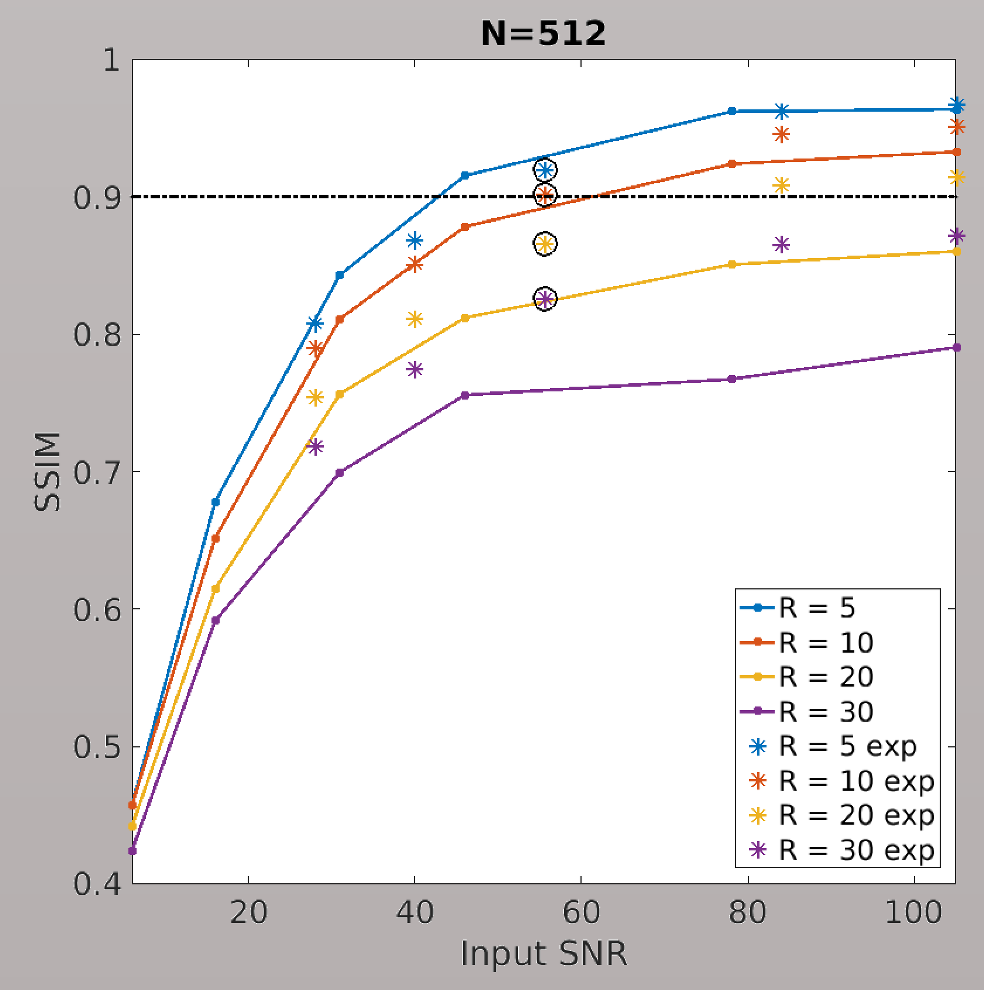

***Figure 2**: Image quality for a constant image size N=512. SSIM evolution in simulations as a function of input SNR for acceleration factors R of 5, 10, 20 and 30 (lines). Experimental points obtained on ex-vivo brain baboon on 7T MR scanner (*) were added to the graph. Circled experimental points (○) images are displayed in Fig. 3. The black dashed line indicates a chosen SSIM threshold of 0.9.*

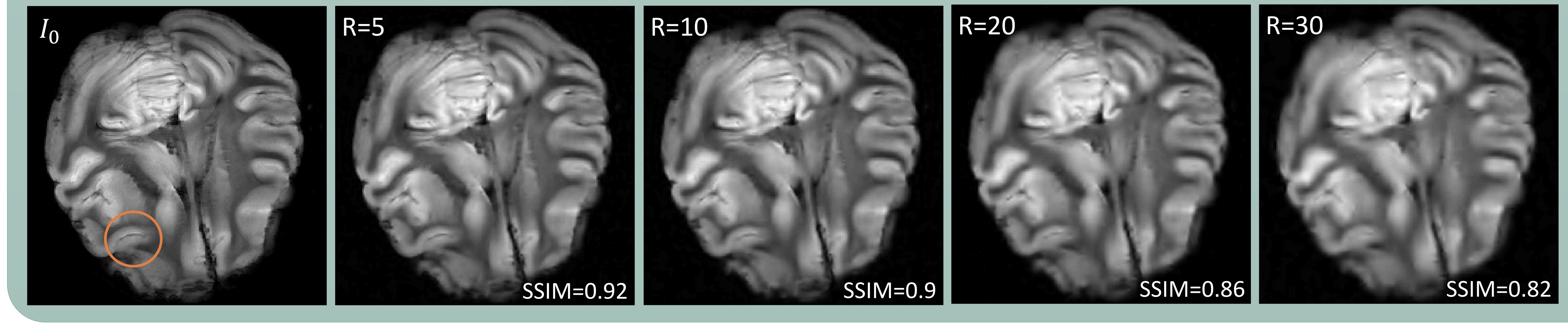

***Figure 3**: Visualization of SSIM scores for N=512 and input SNR=56. Reconstructions are displayed for acceleration factors R of 5, 10 and 30, along with their SSIM scores. The reference I_0 was taken as the fully sampled image of SNR=105. The orange circle on I_0 indicates a region of visible quality loss as R increases.*

CONCLUSIONS

In practice, our study provides CS-MRI users with quantitative guidance in the maximum undersampling factor that should be used to reach a desired image quality, not only based on the image size but also on the available SNR in the original fully sampled image. On the one hand, for a constant input SNR, our simulations showed that the larger the image size, the larger the maximum acceleration factor can be while respecting a targeted image quality. On the other hand, we observed that performances were significantly reduced when the input SNR was decreasing. However, for a given image size, our simulations showed that there is a minimum SNR above which it is possible to reach the desired quality with the maximum undersampling factor. In-house experiments performed on an ex-vivo baboon brain with a 7T scanner corroborated these results quantitatively and suggest that our results could provide classical undersampled MR acquisitions with an upper bound of the maximum usable undersampling factor.

ACKNOWLEDGMENTS

The authors wish to acknowledge Michel Bottlaender for the use of the ex-vivo baboon brain.

REFERENCES

[1] Lustig, M., Donoho, D. and Pauly, J.M., 2007. Sparse MRI: The application of compressed sensing for rapid MR imaging. Magnetic resonance in medicine, 58(6), pp.1182-1195. [2] Chauffert (2015). Compressed sensing along physically plausible sampling trajectories. PhD thesis. Université Paris XI. https://tel.archives-ouvertes.fr/tel-01235202. Section 6.6.2, p.170. [3] Beck, A. and Teboulle, M., 2009. A fast iterative shrinkage-thresholding algorithm for linear inverse problems. SIAM journal on imaging sciences, 2(1), pp.183-202. [4] Wang, Z., Bovik, A.C., Sheikh, H.R. and Simoncelli, E.P., 2004. Image quality assessment: from error visibility to structural similarity. Image Processing, IEEE Transactions on, 13.(4), pp.600-612. [5] http://dsp.rice.edu/software/rice-wavelet-toolbox. [6] https://www-user.tu-chemnitz.de/~potts/nfft